Accepted Manuscript

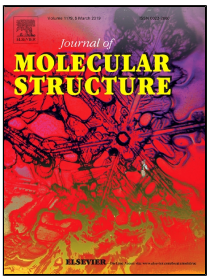

Synthesis, characterization and Biological Investigation of glycine- based sulfonamide derivative and its complex: vibration assignment, HOMO – LUMO analysis, MEP and molecular docking

Parvaneh Shafieyoon, Ebrahim Mehdipour, Y. Sheena Mary

PII:	S0022-2860(18)31500-X
DOI:	10.1016/j.molstruc.2018.12.067
Reference:	MOLSTR 26004
To appear in:	*Journal of Molecular Structure*
Received Date:	08 September 2018
Accepted Date:	16 December 2018

Please cite this article as: Parvaneh Shafieyoon, Ebrahim Mehdipour, Y. Sheena Mary, Synthesis, characterization and Biological Investigation of glycine- based sulfonamide derivative and its complex: vibration assignment, HOMO – LUMO analysis, MEP and molecular docking, *Journal of Molecular Structure* (2018), doi: 10.1016/j.molstruc.2018.12.067

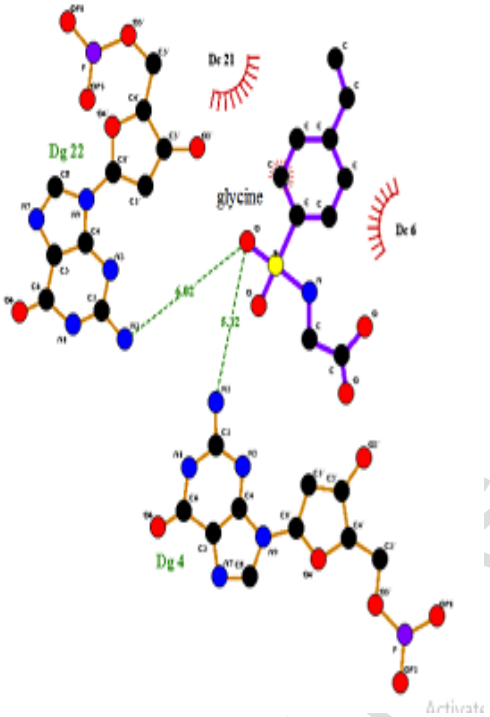

Synthesis, characterization and Biological Investigation of glycine- based sulfonamide derivative and its complex: vibration assignment, HOMO – LUMO analysis, MEP and molecular docking

Parvaneh Shafieyoon, [a] Ebrahim Mehdipour,*[a] Y. Sheena Mary [b]

[a]Department of Chemistry, Faculty of Science, Lorestan University, Khorramabad, Iran.

[b]Department of Physics, Fatima Mata National College, Kollam, Kerala, India.

[a]Corresponding author: Tell: +98-06633120618

E-mail: e_mehdipour@yahoo.com, mehdipour.e@lu.ac.ir

E-mail: parva127@yahoo.com , shafieyoon.pa@fs.lu.ac.ir

E-mail: ysheena@rediffmail.com (Y.S. Mary), sypanicker@rediffmail.com

ABSTRACT

A combined experimental and theoretical investigation has been reported on *N*-(glycine)-*para* styrene sulfonamide (abbreviated as GSS).The GSS and its complex were synthesized for first time in two steps. The GSS was synthesized from the reaction of *para* styrene sulfonyl chloride and glycine in the mild condition. The palladium complex was prepared from the reaction of $PdCl_2$, CH_3CN and GSS as a ligand. The GSS and its complex was confirmed using FT-IR and ^{1}H-NMR spectra. The data obtained from wave number calculations are used to assign vibrational bands obtained in infrared and Raman spectra recorded. Potential energy distribution was done using GAR2PED program. HOMO-LUMO analysis, and Molecular Electrostatic Potential studies of the GSS and its complex have been investigated using DFT method. The GSS is investigated against Staphylococcus aureus and Escherichia coli. Molecular Docking study of GSS is also reported.

Keywords: *N*-(glycine) -*para* styrene sulfonamide; DNA; BSA; HSA; Molecular docking; MEP; PED.

Introduction

Sulfonamide compounds, as antibacterial agents, are extensively applied in the world due to their low toxicity and excellent activity against bacterial diseases[1, 2]. These materials are widely used to prevent the growth of bacteria in the body. Some sulfonamide derivatives in pharmaceutical as antibacterial agents such amino acid, imidazole[3]. In the overall, antimicrobial properties of Sulfonamide derivatives are well known. Therefore, the clinical and medicinal properties of sulfonamide derivatives as antibacterial agent, in a group of commercial pharmaceutical compound have been known. The number of sulfonamide derivatives as an inhibitor to prevent of generation and progression of cancer cells was applied such as tetrahydroquinoline [4]and

chromone[5] containing sulfonamide moiety. During the past two decades, the synthesis of sulfonamide derivatives have been developed as antibacterial and anticancer drugs [6-13].In the recently, by changing the structural parts of sulfonamides, new drugs have been designed. These investigations promoted us to synthesize and evaluate a sulfonamide derivative for pharmaceutical chemistry, we have selected glycine and styrene structural parts to synthesis a new sulfonamide structure due to these group in coordination to metals and synthesis of novel complex-based sulfonamide drugs. In other words, the title compound have medicinal property. In our previous research, we reported the synthesis of sulfonamide and amino acid derivatives [14-16] and theoretical investigation about the new drug-based materials [17, 18]. In this work, the title compound was obtained by the reaction of glycine with para styrene sulfonyl chloride. The bioactivity of this compound for the first time was investigated in vitro against gram positive and gram negative bacteria. Molecular docking calculations were performed to evaluate the medicinal properties of the title compound.

2. Material and methods

Para- styrene sulfonic acid sodium salt, PCl_5, sodium hydroxide, CH_3CN, $PdCl_2$, $CHCl_3$ and glycine were purchased from Aldrich Company and were used without further purification. Fourier transform infrared spectra of prepared compounds were recorded at 400–4000 cm^{-1} region using KBr pellets on Shimadzu FT-IR 8400 spectrometer. ^1H NMR spectrum was recorded on a Brucker Ultrashield 300 MHz spectrometer using D_2O as solvent and tetramethylsilane as internal standard.

2.1. Preparation of Para styrene Sulfonyl Chloride

To prepare the monomer first, *Para*- styrene sulfonyl chloride was synthesized as follows: 7.50 g of PCl_5 (36mmol) was placed in a 500-mL round-bottomed flask, equipped with magnetic stirrer, 5.00 g (24mmol) of *Para*-styrene sulfonic acid sodium salt was added slowly with ice bath cooling.

After 30 min. it was heated under reflux at 50-60°C for 2 hr. The product was cooled and separated from inorganic materials by chloroform and ice water. The chloroform was evaporated from the *Para*- styrene sulfonyl chloride. The product was washed 3 times with water. The solvent was evaporated and product used without further purification. Experimental details are described in Ref [19]

2.2. Preparation of N-(glycine) - Para- styrene sulfonamide (GSS)

The synthetic method for the preparation of the GSS with chemical formula ($C_{10}H_{11}NO_4S$) is as follows: In a 100 mL round-bottomed flask, equipped with magnetic stirrer, 4.86 g *para* vinyl styrene sulfonyl chloride (24 mmol) in 50 mL $CHCl_3$ as a solvent and 1.8 g glycine (24 mmol) were placed. Then, 24 mL NaOH 1M was slowly added. The reaction mixture was stirred for 4 h at room temperature. After the reaction time, the organic layer was separated and GSS as the product was obtained. The obtained product was washed 3 times with $CHCl_3$ and analyzed without further purification (Yield 4.79 g, 83.0%, m.p. 141°C). IR (KBr, Cm^{-1}): 3616(υOH), 3394(υNH), 3050(υCHPh), 3009(υCH, υCH_2), 2975(υCH_2), 2880(υCH_2), 1743(υC=O), 1570(υPh, δCHPh), 1462(δNH, υPh), 1433(δCH_2), 1320(υSO_2, δCH_2), 1245(υCO, δCH_2, δNH), 1136(δCH_2, δOH, υCN), 1082(υCN, υSO_2), 1041(δCH_2, υPh, 1008(δCH_2, δCH, υPh), 910(γCC), 813(γCHPh), 727(τPh, γCC,γCS, γCHPh) 640(τOH, δSO_2, γC=O), 559(γNH, δNH). ^{1}H-NMR ((D_2O, ppm): 2.04(s, CH_2), 3.77(NH) 5.42(CH in vinyl), 5.97(CH in vinyl), 6.81(CH in vinyl), 7.66 (CH Benzene), 7.76 (CH Benzene), 9.95(COOH).

2.3. Preparation of complex ($PdCl_2L$*)*

The synthetic method for preparation of palladium complex is as follows: 0.09 g $PdCl_2$ (0.5 mmol) and CH_3CN (50 mL) were placed in a 100-mL round-bottomed flask equipped with a reflux condenser and a magnetic stirrer. The mixture was stirred and warmed to 70 °C to give a light

orange solution. Then, 0.127 g ligand (0.5 mmol) and sodium hydroxide 0.5 M (2 mL) were added. The reaction mixture refluxed for 12 h and the green solid appeared. The green solution filtered and washed with CH_3CN (3 × 10 mL). The product was used without further purification.

IR (KBr, Cm^{-1}): 3050(υCHPh), 3009(υCH), 2987(υCH_2), 2880(υCH_2), 1743(υC=O), 1510(υPh), 1462(δNH, υPh),, 1433(δCH_2), 1315(υSO_2, δCH_2), 1245(υCO, δCH_2, δNH), 1136(δCH_2, δOH, υCN, 1082(υCN, υSO_2), 1041(δCH_2, υPh, 1008(δCH_2, δCH, υPh), 910(γCC), 813(γCHPh), 727(τPh, γCC, γCS, γCHPh) 640(τOH, δSO_2, γC=O), 559(γNH, δNH). ^{1}H-NMR (D_2O, ppm): 2.04(s, CH2), 5.42(CH in vinyl), 5.97(CH in vinyl), 6.81(CH in vinyl), 7.66 (CH Benzene), 7.76 (CH Benzene),

2.4. Computational details

Calculations of the GSS were performed using Gaussian 09 software[20].These calculations include geometry optimization(opt-freq), MEP, HOMO – LUMO analysis were performed using density functional theory (DFT) [21, 22].The optimization (opt-freq) of compounds was carried out using CAM-B3LYP/Aug.-cc-pVDZ level of theory. The Potential Energy Distribution (PED) of the normal modes among the respective internal coordinates was calculated for GSS using the GAR2PED program [27] and compared with theoretical and experimental values. PASS (Prediction of Activity Spectra) [23]was used as an online server to predict the activity of the ligand. Molecular docking has recently been used as a tool to get an insight into ligand – receptor interaction and screen molecules for the binding affinities against a special receptor. Molecular docking calculations were performed on AutoDock-Vina software[24]. The output of geometry optimization (using CAM-B3LYP/Aug-cc-pVDZ level of theory) for title compound was used as the input of ligand for docking processes. Lamarckian Genetic Algorithm (LGA) available in Autodock was employed for docking, as the most popular algorithm[25, 26]. The 3D crystal

structure of employed DNA, BSA and HSA as receptors were obtained from Protein Data Bank (PDB ID: 423D, 4F5S, 1AO6). The graphical representation of ligand-receptor interaction was obtained using ligplot software [27].

2.5. Antibacterial assays

The minimal inhibitory concentration (MIC) is determined by preparing solutions of the chemical in vitro at increasing concentrations, incubating the solutions with the separate batches of cultured bacteria, and measuring the results using agar solution. It is used to measure the Minimum Inhibitory Concentration [MIC] of an antimicrobial agent, which is the lowest concentration of antibacterial agent which will prevent the growth of bacteria .The MIC of the GSS as antibacterial agent against Escherichia coli and Staphylococcus aureus will be reported in the next section. The GSS was tested for its antibacterial activity against Staphylococcus aureus, as the model from Gram-positive and Escherichia coli as Gram-negative bacteria by the disk diffusion method [28].

2.6. Preparation of Nutrient-Agar medium

For this work, 3.80 g of Nutrient-Agar (NA) medium was dissolved in 100 mL of distilled water. This solution was sterilized at 120 °C for 20 min in an autoclave. Then, 20 mL of this solution was solidified in Petri plate.

3. Result and discussion

3.1. Synthesis and characterization

The synthetic routes for preparation of GSS and its complex, as explained in experimental section, are schematically represented in Schemes1 and 2.

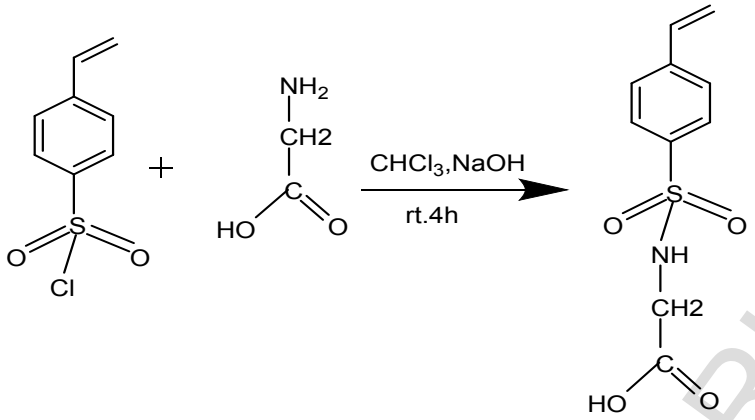

Scheme 1. The reaction involving synthesis of GSS

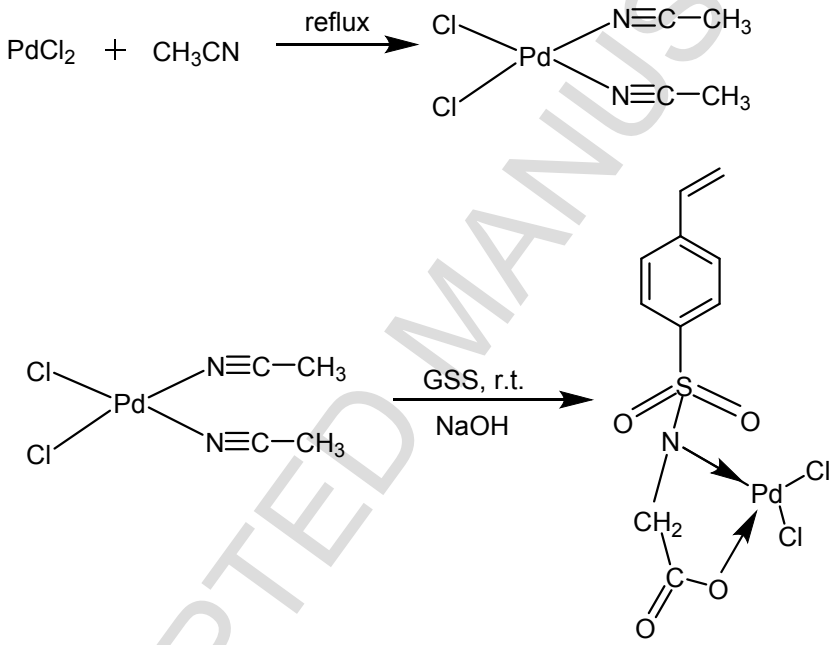

Scheme 2. Synthesis of complex

3.2. Tautomeric and dynamic processes

GSS could be presented in two different tautomers (named as T_1, T_2). This is important to know about the relative stabilities of these tautomers (Fig.1).

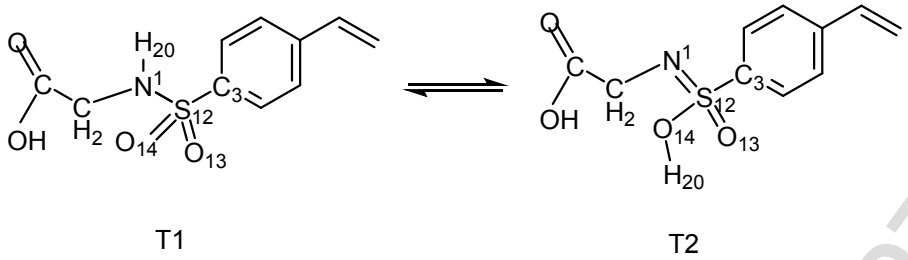

Fig. 1. The general structures of GSS tautomers

In fact, structures of these tautomers were calculated using CAM-B3LYP/Aug.-cc-pVDZ level of theory. Thermodynamic properties such as electronic energies, relative total energies, relative enthalpies, and relative Gibbs free energies for two Tautomers (T_1 and T_2) shown in the Table1, As a result, T_1 tautomer is the more stable due to the symmetrical elements in SO_2.

Table 1. Kinetic and thermodynamic data of two tautomers

Tautomer	Ee	ZPE	Rel.E	Rel.H°$_{298}$	Rel. G°$_{298}$
T_1	-1141.6938	0.202907	-1141.475378	-1141.474433	-1141.536567
T_2	-1141.1358	0.202631	-1140.917449	-1140.916504	-1140.978557

All energetic data have been reported in Hartrees.

3.3 Molecular structural

The optimized geometry (opt-freq) using (CAM-B3LYP method Aug –cc–pVDZ) of GSS was calculated. The numbers of atoms was defined in Fig. 2.

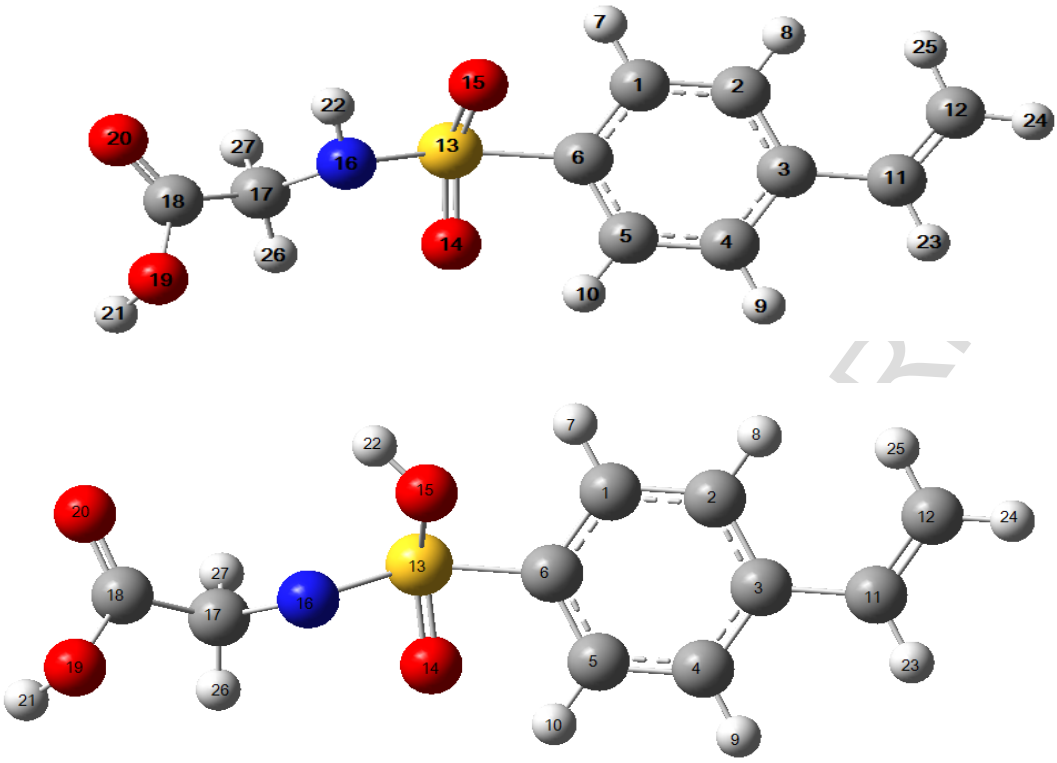

Fig.2.Optimized geometry T_1 (top) and T_2 (bottom) of GSS

3.4. Spectroscopic characterization of GSS

The experimental FT- IR of GSS is reported in experimental section (Fig.3) The C–H stretching frequencies of aromatic can be observed in the range of 3100–3000 cm^{-1} is showed at 3106 cm^{-1}. The aliphatic C–H stretching frequencies are also appeared below 3000 cm^{-1} . The C= C stretching vibration in the range of 1650–1430 cm^{-1} and the C–H bending bands are appeared in the regions 1275–1000 cm^{-1} (in-plane C-H bend) and 900–690 cm^{-1} (out-of plane C-H bend). In addition, the stretching mode of NH group is appeared at 3234cm^{-1}. The out- of –plane NH wag is assigned at 556cm^{-1} in the IR spectrum. In the following discussion, Sulfonamides absorb strongly at 1370-1335 and 1170-1155 cm^{-1} .The stretching mode symmetrical and asymmetrical O=S=O is observed at 1174$cm^{-1}$and 1384 cm^{-1}, respectively.

NH modes

According to literature [29, 30]the NH vibrations are expected in the following regions: stretching mode: 3500-3300 cm^{-1}; deformation modes: around 1500, 1250 and 750-600 cm^{-1}. For the title compound, the NH stretching modes are assigned at 3396 cm^{-1} theoretically (Table 2) and the NH deformations are assigned at 1464, 1279, 561 cm^{-1} theoretically. The reported values of NH modes are at 3462 cm^{-1} in the IR spectrum, 3450 cm^{-1} in the Raman spectrum, 3400 cm^{-1} theoretically (stretching modes), 1508, 1219, 655 cm^{-1} (DFT) (deformation modes[31] and 1587, 1250, 650 cm^{-1} (IR), 1580, 1227, 652 cm^{-1} (DFT) (deformation modes[32].

Phenyl ring vibrations

The phenyl CH stretching modes are assigned at 3079, 3076, 3061, 3049 cm^{-1} theoretically. The phenyl ring stretching modes are assigned at 1569, 1539, 1464, 1372, 1301 cm-1 theoretically[33]. The ring breathing mode of para-substituted phenyl rings with entirely different substituent are expected in the range 780-880 cm^{-1} according to literature[34] and in the present case, this is confirmed by the band at 772 cm-1 theoretically. The phenyl ring breathing mode of para substituted phenyl rings was reported at 795 cm^{-1} [35] at 873 cm^{-1} in the IR spectrum and at 861 cm^{-1} theoretically [36]and at 753 cm^{-1} in IR spectrum, 793, 759 cm^{-1} theoretically[18] The in-plane CH bending modes of the phenyl rings are assigned as 1270, 1161, 1096, 989 cm^{-1} (DFT) as expected[33]. The out-of-plane CH bending modes of the phenyl rings are assigned at 956, 942, 833, 814 cm^{-1} (DFT) for PhIV.

COOH modes

For the title compound, the C=OOH modes are assigned at 3612 cm^{-1} (DFT) (OH stretching mode), 1746 cm^{-1} (DFT) (C=O stretching mode), 603, 502 cm^{-1} (DFT) (C=O deformation modes), 1301, 637 cm^{-1} (DFT) (OH in-plane and out-of-plane deformation), 1248 cm^{-1} (DFT) (C-O stretching) as expected in literature [33]. The reported values are 1680, 561(IR), 1675, 735, 555 (DFT) for

C=O group, 1321 (IR), 1318, 920 (DFT) for OH group and 1235 (IR), 1238 cm^{-1} (DFT) for C-O, for a similar derivative[37].

C=C, and CH_2 modes

For the title compound, C=C stretching mode is assigned at 1617 cm^{-1} (DFT[38]. In the present case, the CH_2 modes are assigned at 3102, 3025, 2974, 2879 cm^{-1} (DFT) (stretching modes), 1435, 1405, 1318, 1201, 1134, 1040, 1007, 974 cm^{-1} (DFT) (deformation modes)[39].

SO_2 modes

The asymmetric and symmetric stretching vibrations of SO_2 are reported in the range 1330 ± 60 and 1180 ± 45 cm^{-1} respectively. For the title compound, the DFT calculations give these modes at 1318 and 1179 cm^{-1}. The SO_2 deformation bands are expected in the regions 535 ± 40, 485 ± 50, 405 ± 65, 320 ± 40 cm^{-1}. DFT calculations give SO_2 modes at 541, 472, 383, 329 cm^{-1} and most of the bands are not pure but contains significant contributions from other modes also. Rodriguez et al [33] reported the SO_2 bands in the range 1242-1394, 590-632 and 460-470 cm^{-1}. The C-S stretching modes are assigned at 630 cm^{-1} theoretically as expected[33].

Table 2. Theoretical (B3LYP/6-311G (d, p)) and experimental IR wavenumbers with PEDs (Vibrational assignments) of the GSS

	Scaled frequency	IR intensity	Observed IR bands	Assignments
75	3612	95.44	3616	υOH(100)
74	3396	81.41	3394	υNH(100)
73	3102	8.96	-	υCH_2(98)
72	3079	1.62	-	υCHPh(92)
71	3076	2.19	-	υCHPh(96)
70	3061	3.25	-	υCHPh(99)
69	3049	9.31	3050	υCHPh(94)
68	3025	2.48	-	υCH_2(83),υCH (15)
67	3016	11.80	3009	υCH(83),υCH_2(16)
66	2974	6.40	2975	υCH_2(97)
65	2879	17.96	2880	υCH_2(97)
64	1746	278.00	1743	υC=O (80)

63	1620	6.56	-	υC=C(60), δCH_2(15), δCH(11)
62	1569	15.89	1570	υPh(56), δCHPh(13)
61	1539	4.46	-	υPh(69)
60	1464	6.73	1462	δNH(59), υPh(35)
59	1435	16.84	1433	δCH_2(90)
58	1405	2.09	-	δCH_2(62), δCH (17)
57	1397	9.50	-	δNH(22), δCH_2(36), υCC(13)
56	1372	20.34	-	υ Ph(42), δCHPh(22)
55	1318	224.25	1320	υSO_2(43), δCH_2 (41)
54	1301	3.25	-	δOH (40), υPh(42)
53	1279	2.25	-	υPh(32), δNH(35)
52	1270	14.86	-	δCHPh(53), υPh(19), υSO_2(10)
51	1261	57.09	-	δCH_2(20), δOH (17), υSO_2(19)
50	1248	63.13	1245	υCO(41),δCH_2(21), δNH (14)
49	1201	15.45	-	δCH_2(87)
48	1179	1.21	-	υSO_2(39),υPh(21)
47	1161	0.76	-	δCHPh(71)
46	1134	143.33	1136	δCH_2(52), δOH(16), υCN(17)
45	1096	30.84	-	δCHPh (48), υPh(24)
44	1085	168.08	-	υCN(33), υSO_2(23)
43	1081	259.37	1082	υCN(28), υSO_2(21)
42	1040	77.82	1041	δCH_2(47), υPh(22)
41	1007	77.82	1008	δCH_2(62), δCH (11), υPh(11)
40	989	7.41	-	υPh(61), δCHPh (47)
39	987	13.97	-	δCH_2(49),γCH(43)
38	974	0.66	-	δCH_2(72), γC=O(19)
37	956	0.23	-	γCHPh(91)
36	942	0.03	-	γCHPh(78),τPh(18)
35	911	43.07	910	γCC(95)
34	886	5.40	-	υCC(31),δCH_2(18), δNH (16), υSN(14)
33	833	25.96	-	γCHPh(65), γCC(12)
32	814	21.01	813	γCHPh(85)
31	812	91.32	-	υSN(36), υCC(25)
30	772	5.82	-	δPh (28), υCC(18), υPh(39)
29	728	0.07	727	τPh(56), γCC(12),γCS(9), γCHPh(11)
28	637	280.98	640	τOH(43), δSO_2(16), γC=O(15)
27	630	10.66	-	τPh(32), γCH(12), υCS(38)
26	625	4.26	-	τOH(22), τPh(42), δPh(16)
25	620	2.42	-	δPh(62)
24	603	37.89	-	δC=O(44)
23	561	109.15	559	γNH(43), δNH(12)
22	541	30.31	-	δSO_2(36), δCC(21), δPh (17)
21	516	59.56	-	δSO_2(22), τPh(18)

20	502	53.65	-	γC=O(38), τOH(22), δCH_2(11)
19	472	36.94	-	δSO_2(37), γNH(15), δC=O(10)
18	462	44.10	-	δCC(37), γNH(18), δC=O(15)
17	443	0.84	-	τPh(36),γCC(17), δSO_2(16)
16	399	0.31	-	τPh(81)
15	383	2.42	-	δSO_2(41), δC=O(17), δCS(15)
14	329	2.82	-	δSO_2(51), γCC(17), τPh(12)
13	308	2.93	-	δSO_2(42), δC=O(18)
12	258	2.33	-	δPh(18), δCC(12), δSO_2(15)
11	234	1.03	-	δSO_2(14), δCC(24)
10	224	1.51	-	δCH_2(12), δCC(18), δSO_2(15)
9	205	0.56	-	δCH_2(18), γCS(12), δSO_2(11)
8	136	1.80	-	δCS(49), δCC(17)
7	123	3.45	-	τC=O(22), γNH(14), τPh(11)
6	107	2.67	-	δNH(28), τNH(18), δCH_2(13), τC=O(12), δSO_2(12)
5	77	2.63	-	τC=O(24), γCS(18), τCH_2(18),τCC(11), δSO_2(10)
4	46	1.64	-	τC=O(41), τNH(35)
3	40	0.52	-	τCC(45), τSO_2(13), τPh(12)
2	36	0.26	-	τSO_2(50), τCC(14)
1	20	0.21	-	τCH_2(48)

Ph-phenyl ring; υ-stretching; δ-in-plane deformation; γ-out-of-plane deformation; τ-torsion
Potential energy distribution is given in brackets in the assignment column.

In order to investigate the performance of vibrational wave numbers of the title compound, the root mean square (RMS) value between the calculated and observed wave numbers were calculated. The RMS values of wave numbers were calculated using the following expression

$$\text{RMS} = \sqrt{\frac{1}{n-1}\sum_i^n (\upsilon_i^{calcu} - \upsilon_i^{exp})^2}$$

The RMS errors of the observed IR bands are found to 1.55. The small differences between experimental and calculated vibrational modes are observed. This is due to the fact that experimental results belong to solid phase and theoretical calculations belong to gaseous phase.

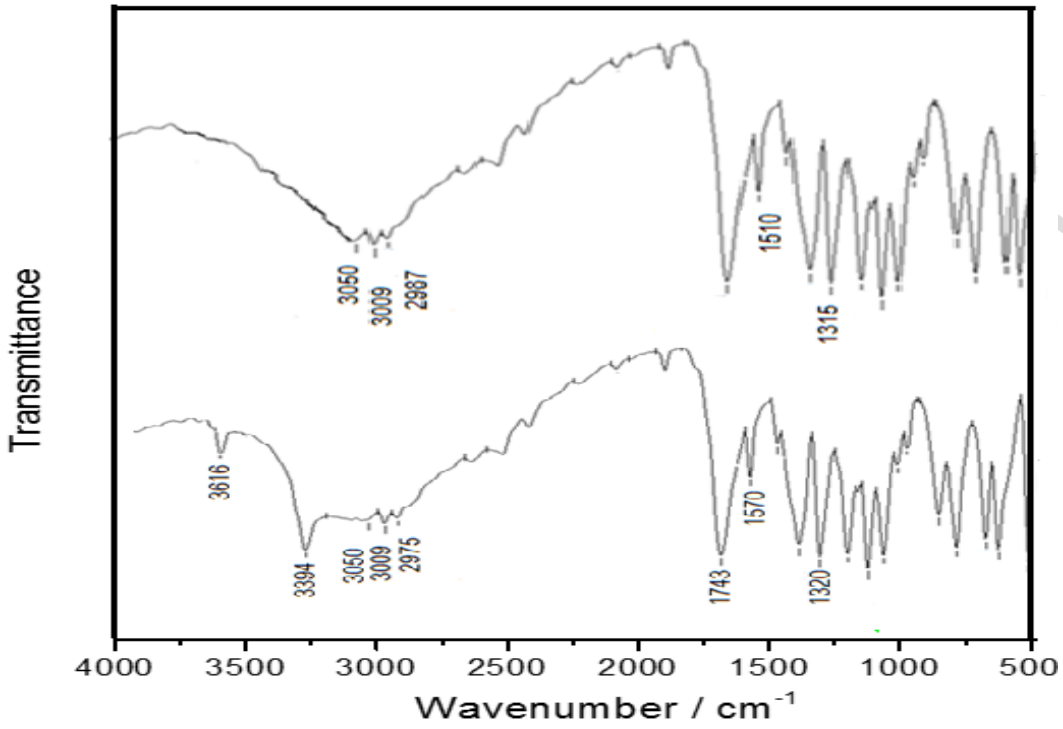

Fig. 3. The experimental FT-IR spectra of GSS (bottom) and complex (top)

3.5. Observed and calculated ^{1}H NMR chemical shifts

The experimental ^{1}H-NMR spectrum of the compound are reported in section 2.2 (Fig.4) The ^{1}H-NMR spectrum of the GSS was recorded in D_2O as solvent with TMS as internal standard at 400 MHz

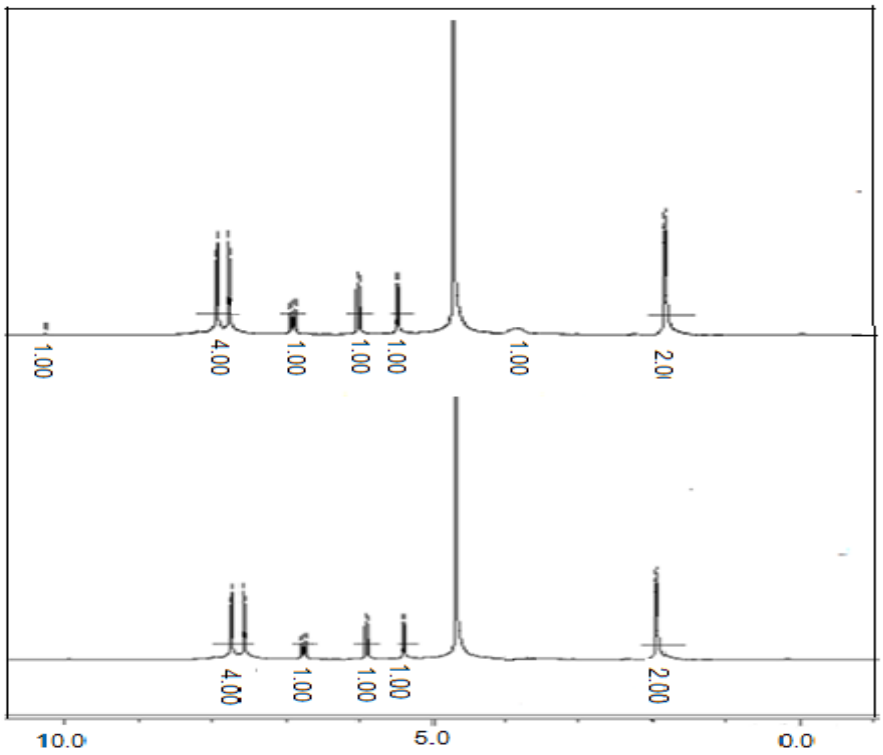

Fig.4.The experimental ^{1}H-NMR spectra of GSS (top) and complex (bottom)

Table 3. Experimental and calculational results related to ^{1}H NMR of ASS

Hydrogen number	exp.	cal.	Hydrogen number	exp.	cal.
8,9	7.66	7.42	24	5.42	5.32
7,10	7.76	7.72	22	3.77	4.18
23	6.81	6.69	21	9.95	5.46
25	5.97	6.00	26,27	2.04	3.01

Observed and computed ^{1}H NMR chemical shifts with their assignments.

The theoretical chemical shift values was calculated by B3LYP method using 6-311+g. The theoretical chemical shift values was calculated by B3LYP method using 6-311+g (2d, p) basis set GIAO model (scale number=0.9614). Then, the results showed that the predicted proton chemical shifts were in good agreement with the experimental data for GSS which represented in Table 3. The RMS error between observed and calculated ^{1}H-NMR are 1.74.The small differences between

experimental and calculated vibrational modes are observed. This is due to the fact that experimental results belong to solid phase and theoretical calculations belong to gaseous phase.

3.6. Spectroscopic characterization of palladium complex

The FT- IR spectrum of complex are listed in experimental section. The vibrational band present at 3396 cm^{-1} is assigned to ν(N–H) for free ligand. This band disappears for the complex because the ligand has been deprotonated. The SO_2 group did not participate in the coordination, then ν_{as}(S=O) shifted from 1320 cm−1 in the free ligand to 1315 cm^{-1} in the complex due to the different spatial orientation of this group in the complex, but the ν_s(S=O) remained almost unchanged. The FT-IR spectrum of ligand showed absorption bands at 1570 cm−1 which was assigned to the ν(C=C) vibrations, in the complex showed 1510 cm^{-1} is correlated with the coordination of the ligands (Fig 3).

3.7. Observed ^{1}H NMR chemical shifts of palladium complex

The experimental ^{1}H-NMR spectrum of the complex is reported in section 2.3. The ^{1}H-NMR spectrum of the compound was recorded in D_2O as solvent with TMS as internal standard at 400 MHz. The ^{1}H-NMR spectrum of the ligand showed a broad singlet at 3.77 ppm for –NH group and 9.95 ppm for –COOH group. The absence of these signals in the spectrum of the complex, due to deprotonation and coordination of anions to palladium and the formation of Pd–N and Pd-O bonds (Fig.4)

3.8. Molecular electrostatic potential

MEP (Molecular electrostatic potential) is as a significant tool to predict the electrophilic and nucleophilic attacks for the biological interactions. The MEP of the title compound was optimized geometry using b3lyp method 6-311+g (d, p) was calculated. As can be observed in Fig.5. The different colors in this plot are indicated different values of the electrostatic potential. Red<orange< yellow<green<blue. The blue illustrate the strongest attraction. The positive area is located around vinyl and phenyl groups. These areas are having positive potential. The negative area is related to C=O group. In these areas having negative potential are over the electronegative atoms such as oxygen. The red indicates the strongest repulsion. These regions of negative potential are associated with the lone pair of electronegative atoms. The residuals species are surrounded by zero potential. The nitrogen of NH and oxygen of OH are as anions coordination to palladium and the formation of complex.

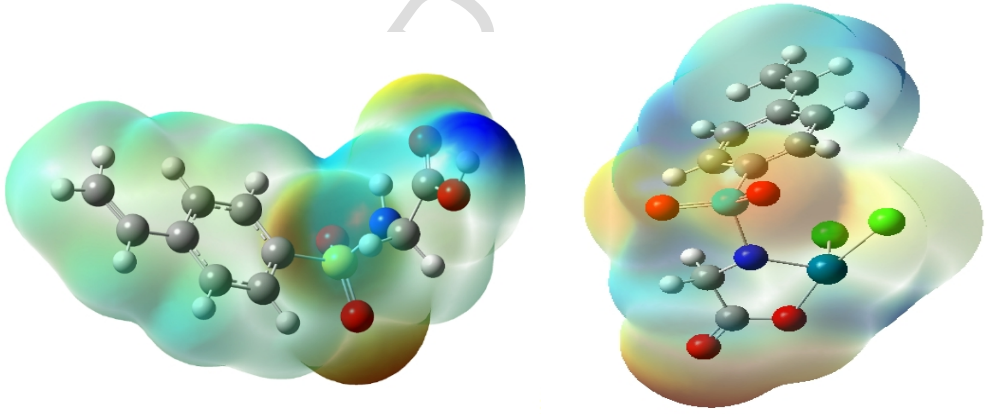

Fig.5. MEP plot of *N*-(glycine) *para* styrene sulfonamide in the left and its complex in the right

3.9. Frontier molecular orbital analysis

Investigation of the HOMO and the LUMO is important in a molecule as a ligand. The LUMO energy explains the ability to accept an electron and the HOMO energy is related to the ability to

donate an electron. Both the HOMO and the LUMO play a significant role in the electrical properties and chemical activities in the compound. The HOMO and LUMO orbital energy are important parameters to predict the chemical properties of the title compound. The HOMO and LUMO orbital energy of GSS and its complex are calculated at the B3LYP method 6-311+g (p,d) basis set. The energy values of the ligand and its complex are, E_{HOMO} = - 6.601,-8.940 and E_{LUMO} = - 5.059,-5.821eV, respectively. The energy difference between the HOMO and LUMO of the ligand and its complex are 1.542 and 3.119 eV, respectively. The energy of HOMO and LUMO orbitals of the GSS and its complex are negative that these compounds are stable and does not decompose spontaneously into theirs elements. According to Parr et al[40]. The molecule with small energy gap is more polarization property, low kinetic stability and is in general called as soft molecule. These molecules can be explained as the resistance towards the deformation of electron cloud and polarization of chemical systems during the chemical process. The chemical softness is a useful concept for predicting the behavior of chemical systems and is related to the stability and low reactivity of a chemical system. The chemical hardness is a useful concept for predicting the behavior of chemical systems and is related to the stability of a chemical system By using HOMO and LUMO orbital energies, the ionization energy and electron affinity of the ligand and its complex can be calculated as: I = - E_{HOMO} = 6.601,8.940 and A = - E_{LUMO} = 5.059, 5.821eV, respectively. The global hardness η and chemical potential μ of the ligand and its complex are given by using the relation $\eta = (I - A)/2$ = 0.771, 1.559 eV, $\mu = -(I + A)/2$= -5.831,-7.381 eV and Electrophilicity index (ω) = $\mu^2/2\eta$ = 22.043, 17.467 eV, respectively. The calculated value describes the catalytically and biologically activity of the title compound (GSS). The atomic orbital components of the frontier molecular orbital are shown in Fig. 6.

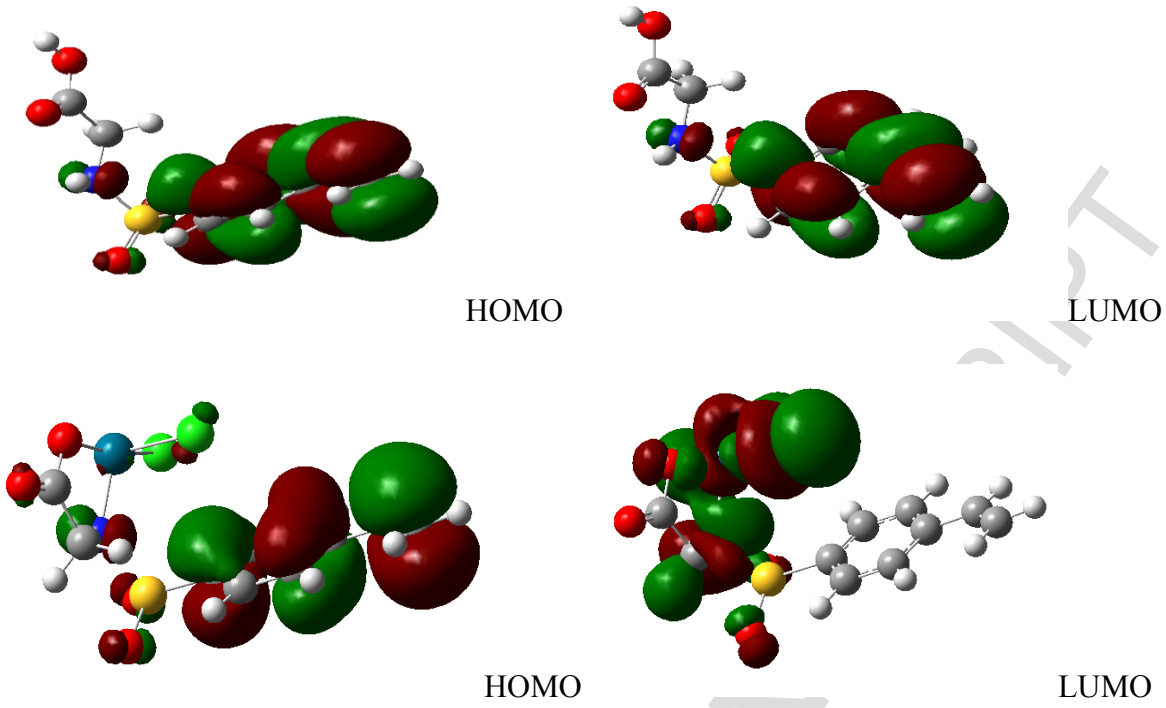

Fig.6. HOMO and LUMO plots of *N*-(glycine) - *para* -styrene sulfonamide in the up and its complex in the down

3.10. Molecular docking studies

We decided to perform molecular docking simulation of the title compound against the 3D crystal structure of DNA, BSA, and HSA were obtained from Protein Data Bank (PDB ID: 423D, 4F5S, 1AO6) respectively. Molecular docking is a significant investigation to understand the ligand-receptor interactions. The ligand was prepared for docking by B3LYP method 6-311+g (p,d)basis set. The active sites of the DNA and BSA were defined to include residues of the active site within the grid box size of 36A°×28A°×20A° for DNA, 82A°×54A°×64A° for BSA and 70A°×54A°×72A° for HSA with a grid-point spacing of 1.00 Å were applied. Among the docked conformations, the best scored conformation predicted by AutoDock scoring function were visualized for ligand-DNA, ligand-BSA, and ligand-HSA interactions in Ligplot and Ligplus software. The resulting docking in which the ligand binds into the DNA creates two hydrogen

bonds (Fig. 7), viz. These hydrogen bonds are between the O_{SO2} of ligand and Dg4 and Dg22 (5.32Å, 6.02Å) respectively. There are hydrophobic contacts between the carbon atom of phenyl ring and Dc6 and Dc21. The BSA creates two hydrogen bonds (Fig.9), viz. These hydrogen bonds are between Oso_2 of ligand with Gly327 and Asp323 (2.96 Å, 3.03 Å) respectively. There are hydrophobic contacts between the carbon atoms and sulfur atom of ligand with Ala212, Leu326, Leu330, Leu346, Ala349, Lys350, and Val481. The HSA creates hydrophobic contacts between the carbon atoms and sulfur atom of ligand with Leu 238, Leu 260, Ile 264, Ile 296, Ala 261 and Ala 291. The binding free energy (ΔG° in kcal mol^{-1}) -6.5 for DNA, -6.8 for BSA and =6.7 for HAS are predicted for the best conformation of the ligand. The values of ΔG° indicate a high binding affinity between DNA, BSA and HSA separately with the ligand (title compound).

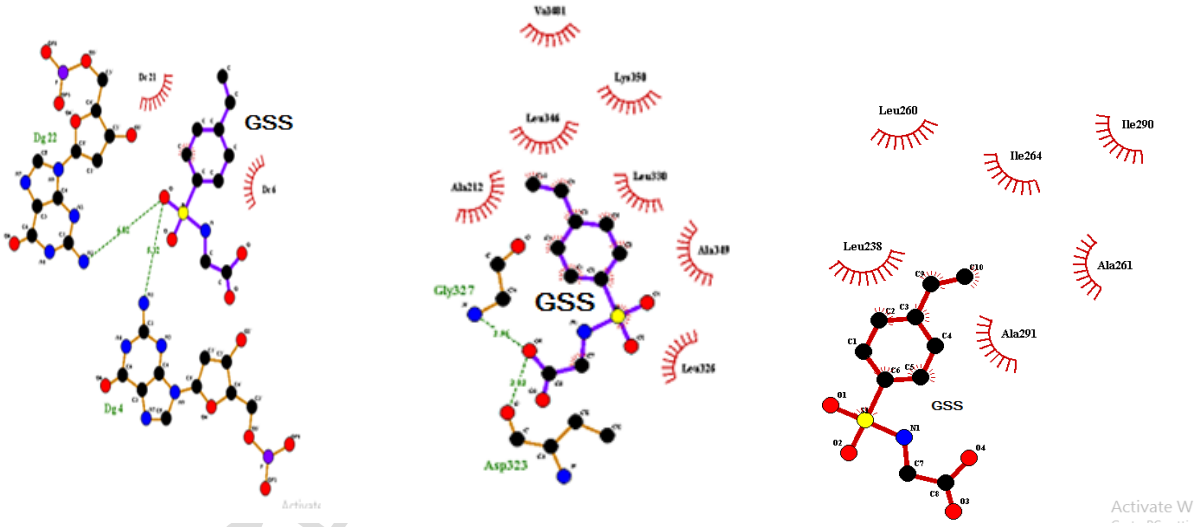

Fig.7. The non-covalent interactions and hydrophobic forces across the binding interface of Ligand–DNA in the left, ligand-BSA in the middle and ligand- HAS in the right (H bonds are shown by green dotted lines).

3.11. The disk diffusion method

A microbial suspension (1 mL) Staphylococcus aureus and Escherichia coli were spread separately over the surface of agar plate, which were then incubated for 24 h at 37°C in an autoclave. Inhibitory zone values (diameter of inhibition) from disk diffusion tests and growth inhibition ring for GSS was reported in Table 4 and Figure 8.

Table 4. Inhibitory zone values (diameter of inhibition) from disk diffusion tests.

Compound	bacteria	Inhibition zone diameter (mm)
N-(glycine)-*para*-styrene sulfonamide	E.coli	19
N-(glycine)-*para*-styrene sulfonamide	S.aureus	21

The results of this assay can be showed that both of Staphylococcus aureus and Escherichia coli are sensitive to *N*-(glycine)-*para*-styrene sulfonamide but Staphylococcus aureus more sensitiveness to the compounds.

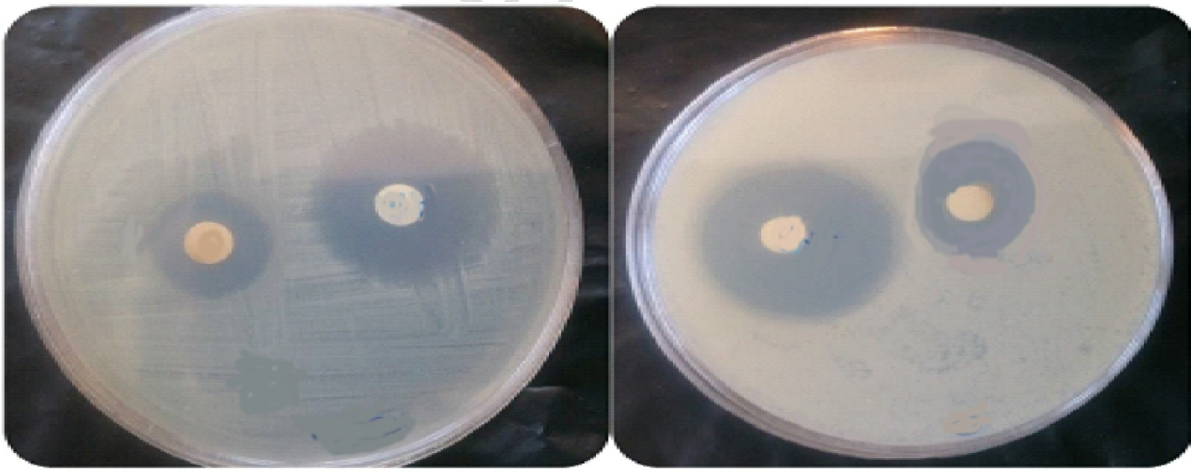

Fig.8 The growth inhibition ring observed for ligand in S.aureus in the right and E.coli in the left.

4. Conclusion

We report the new compounds of based- glycine sulfonamide and its complex. Tautomers of based- glycine sulfonamide were calculated using B3LYP method 6-311+g (p,d) basis set. These calculations were shown the structure of based- glycine sulfonamide is stable. HOMO-LUMO analysis, and Molecular Electrostatic Potential studies of the GSS and its complex have been investigated using DFT method. Molecular electrostatic potential and Frontier molecular orbital analysis were indicated the GSS can be designed for the new catalyst due to its properties. The GSS and palladium complex were characterized using FT-IR and ^{1}H NMR spectra. The Potential Energy Distribution (PED) of the normal modes among the respective internal coordinates was calculated for GSS using the GAR2PED program and compared with theoretical and experimental values. These biological investigations against the Staphylococcus aureus and Escherichia coli and docking simulation of the GSS against the 3D crystal structure of DNA, BSA, and HAS suggest that GSS can be used for the design and synthesis of new based-drug materials

Acknowledgment

We would like to thank Lorestan University for its financial support

Reference

[1] A. Al-Sughayer1, A.Z.A. Elassar, S. Mustafa, F. Al-Sagheer, Synthesis, Structure Analysis and Antibacterial Activity of New Potent Sulfonamide Derivatives J. Biomat. Nanobiotech, 2 (2011) 144-149.

[2] Z.H. Chohan, A. Rauf, M.M. Naseer, M.A. Somra, C.T. Supuran, Antibacterial, antifungal and cytotoxic properties of some sulfonamide-derived chromones, J. Enzyme.Inhib. Med. Chem., 21 (2006) 173-177.

[3] M. M. Ghorab, Z. H. Ismail, A.A. Aziem, S.M. Abdel-Gawad, Antimicrobial activity of amino acid, imidazole, and sulfonamide derivatives of pyrazolo[3,4-d]pyrimidine, Heteroat. Chem., 15 (2004) 57–62

[4] T. Guo, H. Gu, D.W. Hobbs, L.L. Rokosz, T.M. Stauffer, B. Jacob, J.W. Clader, Design, synthesis, and evaluation of tetrahydroquinoline and pyrrolidine sulfonamide carbamates as γ-secretase inhibitors, Bioorg. Med. Chem. Lett., 17 (2007) 3010-3013.

[5] D. H.Nam, K. Y.Lee, C. S.Moon, Y. S.Lee, Synthesis and anticancer activity of chromone-based analogs of lavendustin A, Eur. J. Med. Chem., 45 (2010) 4288-4292.

[6] Z.H. Chohan, M.H. Youssoufi, A. Jarrahpour, T. Ben Hadda, Identification of antibacterial and antifungal pharmacophore sites for potent bacteria and fungi inhibition: Indolenyl sulfonamide derivatives, Eur. J. Med. Chem., 45 (2010) 1189-1199.

[7] A.K. Gadad, C.S. Mahajanshetti, S. Nimbalkar, A. Raichurkar, Synthesis and antibacterial activity of some 5-guanylhydrazone/thiocyanato-6-arylimidazo[2,1-b]-1,3,4-thiadiazole-2-sulfonamide derivatives†, Eur. J. Med. Chem., 35 (2000) 853-857.

[8] M. Ghorab, F. Ragab, H. Heiba, M. El-Gazzar, M. El-Gazzar, Synthesis, in vitro anticancer screening and radiosensitizing evaluation of some new 4-[3-(substituted) thioureido]-N-(quinoxalin-2-yl)-benzenesulfonamide derivatives, Acta. Pharm., 61 (2011) 415-425.

[9] M. Ghorab, F. Ragab, H. Heiba, M. El-Gazzar, S. Zahran, Synthesis, anticancer and radiosensitizing evaluation of some novel sulfonamide derivatives, Eur. J. Med. Chem., 92 (2015) 682-692.

[10] M. M. Ghorab, M. S. Alsaid, M. S. Al-Dosari, M. G. El-Gazzar, M.K. Parvez, Design, Synthesis and Anticancer Evaluation of Novel Quinazoline-Sulfonamide Hybrids, J. Mol., 21 (2016) 1-12.

[11] N. N. Al-Mohammed, Y.Alias, Z Abdullah, R. M. Shakir, E. M. Taha , A. Abdul Hamid, Synthesis and Antibacterial Evaluation of Some Novel Imidazole and Benzimidazole Sulfonamides, Mol., 18 (2013) 11978-11995.

[12] T. Owa, A. Yokoi, K. Yamazaki, K. Yoshimatsu, T. Yamori, T. Nagasu, Array-Based Structure and Gene Expression Relationship Study of Antitumor Sulfonamides Including N-[2-[(4-Hydroxyphenyl)amino]-3-pyridinyl]-4-methoxybenzenesulfonamide and N-(3-Chloro-7-indolyl)-1,4-benzenedisulfonamide, J. Med. Chem., 45 (2002) 4913-4922.

[13] C.T. Supuran, F. Briganti, S. Tilli, W.R. Chegwidden, A. Scozzafava, Carbonic anhydrase inhibitors: Sulfonamides as antitumor agents, Bioorg.Med.Chem., 9 (2001) 703-714.

[14] A.Yari, E. Mehdipour, M. Karami, New bis[N-(4-pyridyl)-P-Toluene Sulfonamide] Palladium Dichloride a Novel Fluorophore for Determination of Lysine Amino Acid, j. Fluoresc., 24 (2014) 1415-1422.

[15] E. Mehdipour, H. Bahrami, Sh. Shamaei, V. Amani, B. Notash, Palladium(II) mixed-ligand complexes containing 2,2'- bipyridine derivaties and 4-toluenesulfonyl-L-serine :synthesis,characterization and crystal structure determination., Phosphorus Sulfur Silicon.. , 190 (2015) 1588.

[16] E. Mehdipour, M. Adeli, M Bavadi, P Sasanpour, B Rashidian, M Kalantari, A Possible Anticancer Drug Delivery System Based on Carbon Nanotube-Dendrimer Hybrid Nanomaterials, J. Mat. Chem., 21 (2011) 15456.

[17] Y.S. Mary, C.Y. Panicker, C. Kavitha, H. Yathirajan, M. Siddegowda, S.M. Cruz, H.I. Nogueira, A.A. Al-Saadi, C. Van Alsenoy, J.A. War, Spectroscopic investigation (FT-IR, FT-Raman and SERS), vibrational assignments, HOMO–LUMO analysis and molecular docking study of Opipramol, Spectrochim. Acta Part A: Mol. Biomol. Spectrosc., 137 (2015) 547-559.

[18] Y.S. Mary, C.Y. Panicker, M. Sapnakumari, B. Narayana, B. Sarojini, A.A. Al-Saadi, C. Van Alsenoy, J.A. War, H. Fun, Molecular structure, FT-IR, vibrational assignments, HOMO–LUMO analysis and molecular docking study of 1-[5-(4-Bromophenyl)-3-(4-fluorophenyl)-4, 5-dihydro-1H-pyrazol-1-yl] ethanone, Spectrochim. Acta Part A: Mol. Biomol. Spectrosc., 136 (2015) 473-482.

[19] N.Yoda, et al. Based-Catalyzed Polymerization of Aromatic Sulfonamides with an Activated Double Bond, J. Poly. Sci. Part A, 3 (1965) 2229-2242.

[20] M. Frisch, G. Trucks, H. Schlegel, G. Scuseria, M. Robb, J. Cheeseman, G. Scalmani, V. Barone, B. Mennucci, G. Petersson, Gaussian 09, revision D. 01, in, Gaussian, Inc., Wallingford CT, 2009.

[21] A.D. Becke, Density-functional thermochemistry. III. The role of exact exchange, J. Chem.Phys., 98 (1993) 5648-5652.

[22] S. Hirata, H. Torii, M. Tasumi, Density-functional crystal orbital study on the structures and energetics of polyacetylene isomers, Phys.Rev. B, 57 (1998) 11994.

[23] A. Lagunin, A. Stepanchikova, D. Filimonov, V. Poroikov, PASS: prediction of activity spectra for biologically active substances, Bioinform., 16 (2000) 747-748.

[24] A. Vina, Improving the speed and accuracy of docking with a new scoring function, efficient optimization, and multithreading Trott, Oleg; Olson, Arthur J, J. Comput. Chem., 31 (2010) 455-461.

[25] R. Huey, G.M. Morris, A.J. Olson, D.S. Goodsell, A semiempirical free energy force field with charge-based desolvation, J. Comput. Chem, 28 (2007) 1145-1152.

[26] G.t.M. Morris, D.S. Goodsell, R.S. Halliday, R.h. Huey, W.E. Hart, R.K. Belew, A.J. Olson, Automated docking using a Lamarckian genetic algorithm and an empirical binding free energy function, J. Comput. Chem., 19 (1998) 1639-1662.

[27] A.C. Wallace, R.A. Laskowski, J.M. Thornton, LIGPLOT: a program to generate schematic diagrams of protein-ligand interactions, Protein engineering, 8 (1995) 127-134.

[28] NCCLS, Methods for dilution antimicrobial susceptibility test for bacteria that grow aerobically, M7-A4, in 1997.

[29] L.J. Bellamy, The Infrared Spectrum of Complex Molecules,, 1975.

[30] N.B. Colthup, L.H. Daly, S.E.Wiberly, Introduction of Infrared and Raman Spectroscopy, Academic Press, New York, 1975.

[31] S.R. Sebastian, M.A. Al-Alshaikh, A.A. El-Emam, C.Y. Panicker, J. Zitko, M. Dolezal, C. VanAlsenoy, Spectroscopic, quantum chemical studies, Fukui functions, in vitro antiviral activity and molecular docking of 5-chloro-N-(3-nitrophenyl) pyrazine-2-carboxamide, J. Mol. Struct., 1119 (2016) 188-199.

[32] Y.S. Mary, H.T. Varghese, C.Y. Panicker, M. Dolezal, Vibrational spectroscopic studies and ab initio calculations of a substituted amide of pyrazine-2-carboxylic acid—C 12 H 10 ClN 3 O, Spectrochim. Acta Part A: Mol. Biomol. Spectrosc., 71 (2008) 725-730.

[33] N.P. Roeges, A guide to the complete interpretation of infrared spectra of organic structures, Wiley, 1994.

[34] G. Varsányi, Assignments for vibrational spectra of seven hundred benzene derivatives, Halsted Press, 1974.

[35] Y.S. Mary, C.Y. Panicker, M. Sapnakumari, B. Narayana, B. Sarojini, A.A. Al-Saadi, C. Van Alsenoy, J.A. War, FT-IR, NBO, HOMO–LUMO, MEP analysis and molecular docking study of 1-[3-(4-Fluorophenyl)-5-phenyl-4, 5-dihydro-1H-pyrazol-1-yl] ethanone, Spectrochim. Acta Part A: Mol. Biomol. Spectrosc., 136 (2015) 483-493.

[36] C.Y. Panicker, K. Ambujakshan, H.T. Varghese, S. Mathew, S. Ganguli, A.K. Nanda, C.V. Alsenoy, FT-IR, FT-Raman and DFT calculations of 3-{[(4-fluorophenyl) methylene] amino}-2-phenylquinazolin-4 (3H)-one, J. Raman Spectrosc., 40 (2009) 527-536.

[37] R. Raju, C.Y. Panicker, P.S. Nayak, B. Narayana, B. Sarojini, C. Van Alsenoy, A.A. Al-Saadi, FT-IR, molecular structure, first order hyperpolarizability, MEP, HOMO and LUMO analysis and NBO analysis of 4-[(3-acetylphenyl) amino]-2-methylidene-4-oxobutanoic acid, Spectrochim. Acta Part A: Mol. Biomol. Spectrosc., 134 (2015) 63-72.

[38] G. Scorates, Infrared characteristics group frequencies, John Wiley and sons, Ltd: Chichester, (1994).

[39] R.M. Silverstein, G.C. Bassler, T.C. Morril, Spectrometric Identification of Organic Compounds,, 1991.

[40] R.G. Parr, L.v. Szentpaly, S. Liu, Electrophilicity index, J. Am. Chem. Soc. 121 (1999) 1922-1924.

We report the new compounds of based- glycine sulfonamide and its complex. These biological investigations and docking simulation of the GSS against the 3D crystal structure of DNA, BSA, and HAS suggest that GSS can be used for the design and synthesis of new based-drug materials